Swift heavy ion induced modification in Ti/Si system studied with sub-nanometre resolution

Swift heavy ion induced modification in Ti/Si system studied with sub-nanometre resolution

Parasmani Rajput[1], **Ajay Gupta**[1,3], **V R Reddy**[1], **Vasant Sathe**[1] **and D K Avasthi**[2]

[1] UGC-DAE Consortium for Scientific Research, University Campus, Khandwa Road, Indore 452 017, India
[2] Inter University Accelerator Centre, Aruna Asaf Ali Marg, New Delhi 110 067, India

E-mail: agupta@csr.ernet.in

Abstract
Swift heavy ion irradiation induced intermixing in Si/Ti thin films has been studied using x-ray waveguide structures. The tri-layer Si/Ti/Si embedded in a planar waveguide provides detailed information about the depth distribution of Ti layer through x-ray fluorescence measurement. Raman spectroscopy shows that the Si layers are amorphous in nature. Quantitative information about the amount of mixed Si as a function of irradiation fluence is obtained from the intensity of the Raman peaks. It is found that the Ti layer gets significantly mixed with Si and at the same time the position of the Ti layer exhibits a small shift towards the surface. Comparison with the results in other metal/silicon systems suggests that the shift of the position of the marker layer is correlated with the sensitivity of the metal layer to electronic energy loss, as envisaged in the thermal spike model. An asymmetric mixing at the two interfaces may be a possible cause of this observed shift.

1. Introduction

In recent years swift heavy ion (SHI) irradiation has been used for controlled modification of the properties of thin-film and multilayer structures [1, 2]. The passage of swift heavy ions (having kinetic energies in the range of MeV/amu) in materials mainly produces electronic excitation of the atoms in the target. Part of this energy gets transferred to the atomic motions via electron–phonon coupling, which may result in material modification [3]. In metallic systems, SHIs are known to produce damage above a certain threshold electronic energy loss, S_{ecr}, which varies significantly from metal to metal [3, 4]. Metals like W and Ag are rather insensitive to electronic energy loss, while metals like Ti and Zr are highly sensitive and Fe and Co show

[3] Author to whom any correspondence should be addressed.
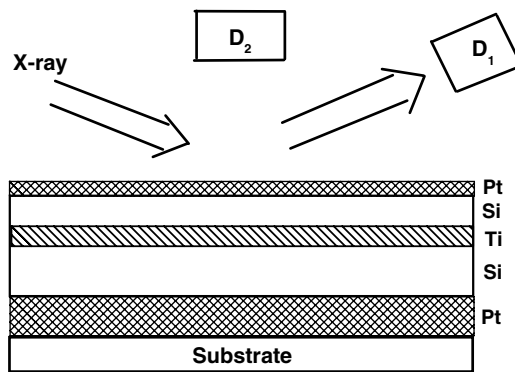
Figure 1. Sketch of the experimental geometry used in the present work. D_1 is a scintillation detector for x-ray reflectivity, D_2 is an energy-dispersive detector for fluorescence measurement. The structure of the waveguide specimen is: substrate (float glass)/Pt (70 nm)/Si (16 nm)/Ti (3 nm)/Si (8 nm)/Pt (2 nm). One may note that the Ti layer is placed asymmetrically with respect to the centre of the cavity formed by the two Pt layers.

intermediate sensitivity to electronic energy loss, S_e [3, 4]. Since, for S_e values close to the threshold, the induced modifications are expected to be small, highly sensitive techniques are needed in order to detect this small change occurring in the system [5].

X-ray waveguide structures have attracted considerable interest because of the possibility of using them for the study of the structural properties of the guiding layer itself [5–9]. In the present work, we use an x-ray waveguide structure to study the changes occurring in a Si/Ti/Si tri-layer upon irradiation with 120 MeV Au ions. Results are compared with irradiation effects in other metal/silicon (metal = Fe, W) systems with different sensitivity to electronic energy loss [5, 10, 11]. The tri-layer Si/Ti/Si embedded in a planar waveguide can provide detailed information about the position and thickness of the Ti marker layer with sub-nanometre resolution using x-ray fluorescence measurements [5].

2. Experimental details

A multilayer with a nominal structure: substrate (float glass)/Pt (70 nm)/Si (16 nm)/Ti (3 nm)/Si (8 nm)/Pt (2 nm), was deposited using ion beam sputtering. The base pressure in the chamber was 1.5×10^{-7} Torr. Two Pt layers form the walls of the planar waveguide, while the tri-layer Si/Ti/Si forms the cavity of the planar waveguide (figure 1). Waveguide modes can be excited in the cavity, whenever the following condition is satisfied:

$$D = n\lambda/2\sin\theta,$$

where λ is the wavelength of the x-rays, θ is the angle of incidence of the x-rays, D is the thickness of the waveguide cavity, and n is the order of the mode [12]. The Ti fluorescence exhibits peaks at angles of incidence corresponding to the waveguide modes due to resonance enhancement of the x-ray intensity inside the cavity. As shown earlier [5], the relative intensities of various peaks depend up on the exact position and width of the Ti marker layer, and the sensitivity of the technique is enhanced by positioning the Ti layer asymmetrically with respect to the centre of the cavity (figure 1). X-ray reflectivity and x-ray fluorescence measurements were performed using a Bruker AXS D8 Advance diffractometer using Cu Kα radiation. The geometry of the experimental setup is shown in figure 1. Reflected x-rays were collected using a scintillation detector, while the Ti Kα fluorescence from the sample was
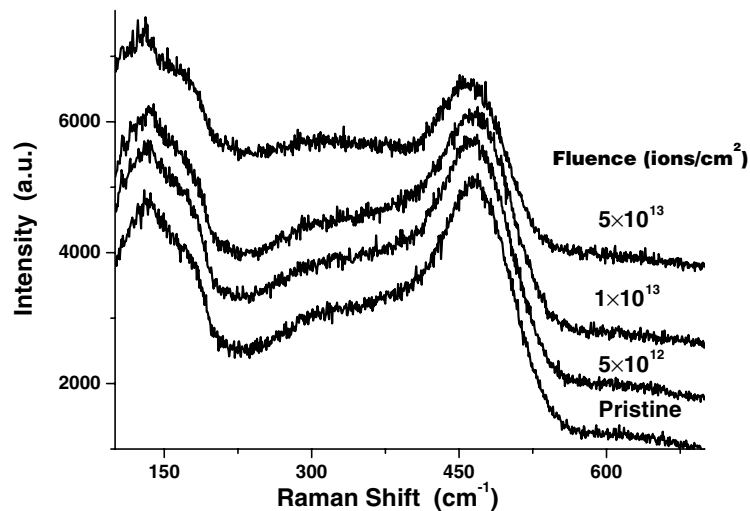
Figure 2. Raman spectra of pristine and irradiated films. The spectra for the different fluences have been shifted vertically for the sake of clarity.

measured using an Amptek XR100T PIN diode detector (with an energy resolution of 250 eV) kept vertically above the sample. Samples were irradiated with 120 MeV Au ions to fluences ranging from 5×10^{12} to 5×10^{13} ions cm^{-2} using the 15UD Pelletron at Inter-University Accelerator Centre (IUAC), New Delhi, India. Raman measurements were performed on a Horiba JY HR800 micro-Raman system using an argon 488 nm laser as an excitation source and a CCD detector.

3. Results and discussions

Figure 2 gives the normalized Raman spectra of the pristine and irradiated films in the spectral range 100–700 cm^{-1}. The spectra for different samples are shifted vertically for clarity. The Raman spectra of all four samples exhibit four distinct features: a broad peak around 465 cm^{-1}, two rather overlapping peaks around 135 and 175 cm^{-1}, and a broad feature around 310 cm^{-1}. The peak around 135 cm^{-1} matches that of platinum silicide [13, 14], while that around 175 cm^{-1} may be attributed to titanium silicide [15]. The broad peak at 465 cm^{-1} matches rather well with that of amorphous Si [15]. The broad feature around 310 cm^{-1} is a second-order acoustic phonon scattering due to Si [16]. With increasing irradiation fluence, the height of the Si peak at 465 cm^{-1} keeps on decreasing, indicating intermixing of Si with Ti. The broad hump near 310 cm^{-1}, which is attributed to second-order acoustic phonon scattering due to Si, also decreases due to irradiation, which is in line with the arguments for decreasing the 465 cm^{-1} feature. The peak around 135 cm^{-1} suggests that, even in a pristine sample, some platinum silicide is formed. However, irradiation does not result in any measurable increase in the platinum silicide peak, which is expected as Pt is known to be highly insensitive to SHI irradiation [3, 4]. The intensity of the Si peak at 465 cm^{-1} has been used to obtain quantitative information about the intermixing. At the highest fluence of 5×10^{13} ions cm^{-2}, more than 30% of the Si gets intermixed with the Ti layer.

Figure 3 gives the x-ray reflectivity of the pristine sample as well as the irradiated samples to fluences of 5×10^{12} and 1×10^{13} ions cm^{-2}. Three sharp dips in the x-ray reflectivity patterns between the critical angles (θ_c) of Si and Pt indicate the excitation of the TE$_0$, TE$_1$ and TE$_2$
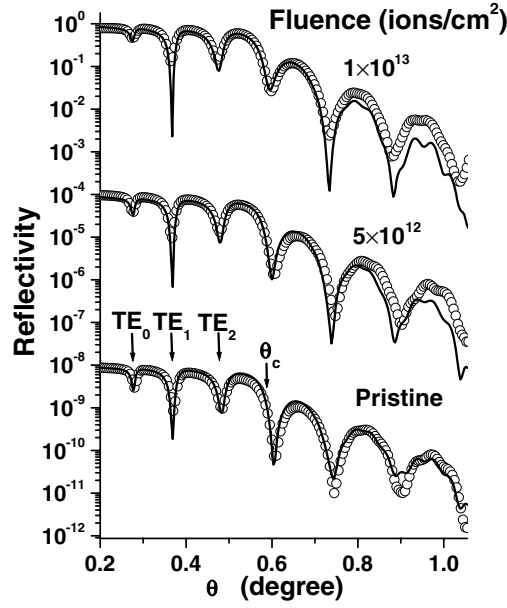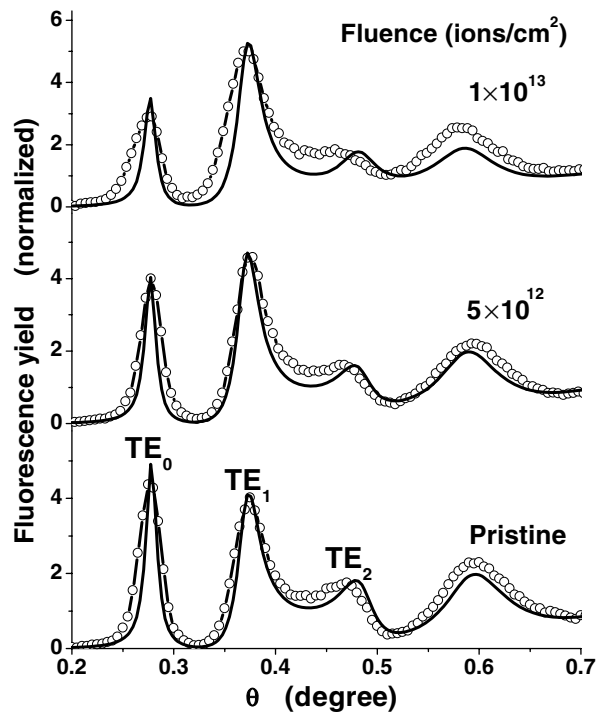
Figure 3. X-ray reflectivity of pristine and irradiated samples as a function of angle of incidence (θ). The arrows indicate that the θ values correspond to the excitation of TE_0, TE_1 and TE_2 modes. The position of the critical angle θ_c, for total reflection from Pt, is also indicated.

modes of the waveguide. The continuous curve denotes the fit to the reflectivity data obtained using Parratt's formulism [17]. The layer thicknesses and interface roughness have been taken as fitting parameters. The fitting of the x-ray reflectivity shows that, while the simulated pattern is sensitive to the total thickness of the cavity plus the top Pt layer, as well as to the interface roughnesses, it is not very sensitive to the position and width of the Ti marker layer. Figure 4 gives the x-ray fluorescence from the Ti marker layer for a pristine sample as well as the samples irradiated to fluences of 5×10^{12} and 1×10^{13} ions cm^{-2}. Fluorescence peaks corresponding to all three modes are visible. The intensity of the x-ray fluorescence, $I(\theta)$, from the Ti layer corresponding to a given angle of incidence can be written as:

$$I(\theta) = C \int I(\theta, z) f(z) \, \mathrm{d}z$$

where C is a normalization constant, $f(z)$ is the concentration profile of Ti, and $I(\theta, z)$ is the depth-dependent x-ray intensity for a given angle of incidence θ. The x-ray intensity inside the multilayer structure was calculated using Parratt's formalism [17, 18]. In figure 4, the continuous curves represent the best-fit results obtained by simultaneous fitting of the reflectivity and fluorescence data. The results of fitting for pristine and irradiated samples are given in table 1. Possible intermixing at various interfaces induced due to irradiation is in general manifested in terms of an increased interface roughness. Since the intermixing of the Ti layer with Si is very strong, it was taken into account by assuming a change in its composition (i.e. a decrease in its electron density) accompanied by a proportional increase in its effective thickness. The resulting electron density profiles are shown in figure 5 [17]. It may be noted that fitting of the observed relative intensity of the fluorescence peaks corresponding to TE_1 and TE_2 modes provides a sensitive way of measuring the position of the marker layer and any shift in the same due to subsequent sample treatment [5]. The intensity of the fourth peak does not match very well with the theory. This may be because of the fact that in the present samples
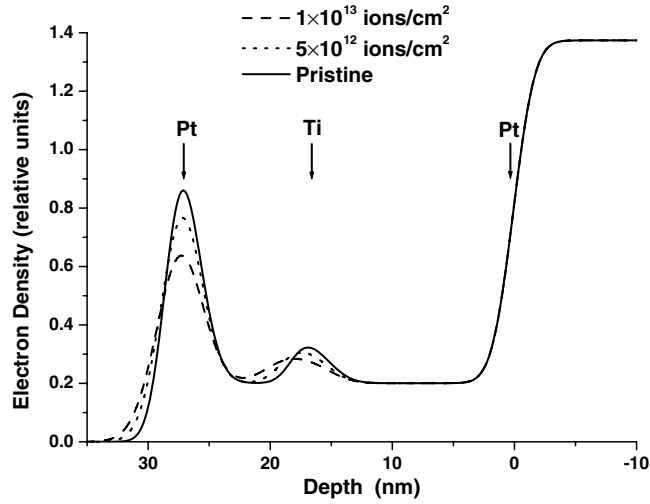
Figure 4. Ti fluorescence from pristine and irradiated samples as a function of scattering vector q.

Table 1. The results of simultaneous fitting of x-ray reflectivity and x-ray fluorescence data for pristine and irradiated samples. The given roughness is that of the top surface of a layer.

Layer	Pristine		5×10^{12} ions cm^{-2}		1×10^{13} ions cm^{-2}	
	Thickness (nm)	Roughness (nm)	Thickness (nm)	Roughness (nm)	Thickness (nm)	Roughness (nm)
Pt	2.2 ± 0.1	1.2 ± 0.05	2.2 ± 0.1	1.6 ± 0.05	2.0 ± 0.1	1.9 ± 0.05
Si	7.9	1.5	7.0	1.5	6.0	1.7
Ti	3.0	1.0	3.8	1.2	5.0	1.5
Si	15.2	1.5	15.3	1.5	15.1	1.7
Pt	70.5	1.4	70.5	1.4	70.5	1.4
Substrate	—	1.0	—	1.2	—	1.2

the position of the fourth peak happens to lie close to the critical angle of Pt, and therefore its intensity would be very sensitive to small variations in the parameters of the Pt layer.

From figure 5, one may note that the Ti layer depth profile broadens considerably with irradiation fluence. At the same time, centroids of the peak exhibits a small shift towards the surface. The profile of the top Pt layer also exhibits a small broadening, which may be partly due to surface roughness and partly due to some intermixing with Si. Surface roughening of films due to swift heavy ion irradiation has been observed in several studies [19]. Swift heavy ion irradiation is known to create damage in metallic systems above a threshold value of electronic energy loss. From the literature, S_{ecr} in Ti and Si is 11 and 13 keV nm^{-1}, respectively, while S_e of 120 MeV Au ions in Ti and Si as calculated using SRIM code [20] comes out to be 23.6 and 12.9 keV nm^{-1}, respectively. Thus S_e in Ti is above the threshold value and

Figure 5. The electron density profile of pristine and irradiated samples as obtained from simultaneous fitting of x-ray reflectivity and Ti fluorescence data.

Table 2. S_{ecr} is the expected threshold electronic energy loss for the creation of defects, as taken from [3]. S_e is the experimental value of electronic energy loss in the metal layer used in the present work and in [5]. The last column gives the shift of the centroid of the metal layer as a percentage of the total thickness of the waveguide cavity.

Marker layer	S_{ecr} (keV nm^{-1})	S_e (keV nm^{-1})	Percentage shift (%)
W	>80	35.4	0
Fe	41	30.4	1.2
Ti	11	23.6	3.4

therefore one expects large damage creation in Ti layer, which would result in intermixing with Si. However, in this model one cannot understand the shifting of the Ti layer towards the surface. In earlier studies [5] a similar shift of a thin layer of Fe in Si was observed due to irradiation by 100 MeV Au ions. Table 2 summarizes the results of irradiation of a Si/M/Si system (where M = W, Fe, Ti). One may note that the shift in the centroid of the metal layer is not correlated with the actual S_e value in the same, as S_e in W is highest, while in Ti it is lowest. However, one can find a positive correlation between the shift and the S_e value normalized to the threshold electronic energy loss S_{ecr} of that element. Since a lower electronic energy loss value means a more efficient energy transfer from the electronic system to the lattice (due to electron–phonon coupling), the shift in the centroid of the layer is correlated with the energy transferred to the lattice. Thus a comparison of the results for M = W, Fe and Ti suggests that the shift in the centroids is correlated with the efficiency of mixing. A possible reason for this shift can be an asymmetric mixing at the two interfaces. In case the mixing at the Si-on-M interface is more compared to that at the M-on-Si interface, intermixing would result in an upward shift of the centroid of the M layer. Other possible reasons could have been a depth-dependent densification of the Si layer. However, this possibility can be ruled out due to the facts that (i) densification of the Si layer takes place in both the Fe/Si and W/Si systems, but upward shifting takes place only in the Fe/Si system, and (ii) in the Ti/Si system no densification of the Si layer takes place, yet shifting of the Ti layer is observed. A hammering effect of the

swift heavy ions [21, 22] could also be a possible reason. However, in that case the effect would have been present in all three cases. In fact, it should have been more in the case of W/Si, since S_e in W is the highest. Thus, an asymmetric intermixing at the interfaces seems to be the most probable cause of the observed shift of the centroid of the Ti layer. It may be noted that asymmetry of the interfaces in multilayers has been observed in several studies in as-deposited films as well as films irradiated with heavy ions ranging in energy from eV to keV [23–26]. Present studies suggest that, even at ion energies of ∼100 MeV, intermixing at the interfaces may be asymmetric.

4. Conclusion

Swift heavy ion irradiation induced intermixing has been studied in the Ti/Si system with sub-nanometre depth resolution using Raman scattering and x-ray standing wave analysis. Raman spectroscopy has been used to get quantitative information about silicide formation. Significant intermixing takes place as a result of irradiation. At the same time, x-ray standing wave analysis gives a clear indication that the metal layer exhibits a small upward shift. A possible reason for this shift can be an asymmetric mixing at the two interfaces of the metal layer.

Acknowledgment

References

[1] Mahnke H E 2004 *Nucl. Instrum. Methods Phys. Res.* B **225** 160
    Bolse W 2003 *Radiat. Meas.* **36** 597
[2] Schiwietz G, Luderer E, Xiao G and Grande P L 2001 *Nucl. Instrum. Methods Phys. Res.* B **175** 1
    Gupta A 2000 *Vacuum* **58** 16
[3] Wang Z G, Dufour Ch, Paumier E and Toulemonde M 1994 *J. Phys.: Condens. Matter* **6** 6733
[4] Dunlop A, Lesueur D, Legrand P, Dammak H and Dural J 1994 *Nucl. Instrum. Methods Phys. Res.* B **90** 330
[5] Gupta A, Rajput P, Saraiya A, Reddy V R, Gupta M, Bernstorff S and Amenitsch H 2005 *Phys. Rev.* B **72** 75436
[6] Zwanenburg M J, Peters J F, Bongaerts J H H, de Vries S A, Abernathy D L and van der Veen J F 1999 *Phys. Rev. Lett.* **82** 1696
[7] Zwanenburg M J, Bongaerts J H H, Peters J F, Riese D O and van der Veen J F 2000 *Phys. Rev. Lett.* **85** 5154
[8] Salditt T, Pfeiffer F, Perzl H, Vix A, Mennicke U, Jarre A, Mazuelas A and Metzger T H 2003 *Physica* B **336** 181
    Pfeiffer F, Mennicke U and Salditt T 2002 *J. Appl. Crystallogr.* **35** 163
[9] Zheludeva S, Kovalchuk M and Novikova N 2001 *Spectrochim. Acta* B **56** 2019
[10] Gupta A, Meneghini C, Saraiya A, Principi G and Avasthi D K 2003 *Nucl. Instrum. Methods Phys. Res.* B **212** 458
[11] Srivastava S K, Avasthi D K, Assmann W, Wang Z G, Kucal H, Jacquet E, Carstanjen H D and Toulemonde M 2005 *Phys. Rev.* B **71** 193405
[12] Fang Y P, Sinha S K, Deckman H W, Hastings J B and Siddons D P 1993 *Phys. Rev. Lett.* **71** 537
[13] Nemanich R J, Sigmon T W, Johnson N M, Moyer M D and Lau S S 1981 *Laser and Electron-Beam Solid Interactions and Materials Processing* ed J F Gibbons, L D Hess and T W Sigmon (New York: North-Holland) p 541
[14] Tsang J C, Matz R, Yokota Y and Rubloff G W 1984 *J. Vac. Sci. Technol.* A **2** 556
[15] Nemanich R J, Fulks R T, Stafford B L and Vander Plas H A 1985 *J. Vac. Sci. Technol.* A **3** 938
[16] Tsang J C, Yokota Y, Matz R and Rubloff G 1984 *Appl. Phys. Lett.* **44** 430
[17] Parratt L G 1954 *Phys. Rev.* **95** 359
    Braun C 1997–99 *The Reflectivity Tool of Parratt32 Version 1.5* HMI Berlin
    de Boer D K G 1991 *Phys. Rev.* B **44** 498
    Nevót L and Croce P 1980 *Rev. Phys. Appl.* **15** 761
[18] Dev B N, Das A K, Dev S, Schubert D W, Stamm M and Materlik G 2000 *Phys. Rev.* B **61** 8462

[19] Avasthi D K, Ghosh S, Ganesa V, Gupta A, Mieskes H D, Huber H and Assmann W 1998 *Appl. Phys.* A **66** S1137
Crespo-Sosa A, Schaaf P, Bolse W, Lieb K P, Gimbel M, Geyer U and Tosello C 1996 *Phys. Rev.* B **53** 14795
[20] Ziegler J F, Biersack J P and Littmark U 1985 *The Stopping and Ranges of Ions in Solids* vol 1 (New York: Pergamon)
[21] Bolse W 2006 *Nucl. Instrum. Methods Phys. Res.* B **244** 8
[22] Hedler A, Klaumünzer S and Wesch W 2006 *Nucl. Instrum. Methods Phys. Res.* B **242** 85
[23] Buchanan J D R, Hase T P A, Tanner B K, Chen P J, Gan L, Powell C J and Egelhoff W F Jr 2002 *Phys. Rev.* B **66** 104427
[24] Bigault T, Bocquet F, Labat S, Thomas O and Renevier H 2001 *Phys. Rev.* B **64** 125414
[25] Süle P, Menyhárd M, Kótis L, Lábár J and Egelhoff W F Jr 2005 *Preprint* cond-mat/0510077v1
[26] Devolder T 2000 *Phys. Rev.* B **62** 5794